Spatial Resolution Improvement of Seasonal Evapotranspiration for Irrigated Rice, Zhanghe Irrigation District, Hubei Province, China

Y. Chemin[1] and T. Alexandridis[2]

[1] RS & GIS FoS, Asian Institute of Technology, P.O. Box 4 Klong Luang, 12120 Pathumthani, Thailand
Tel: +66 2 516 0110 – 44 Fax: +66 2 516 2126 E-mail: yann.chemin@ait.ac.th

[2] Faculty of Agriculture, Aristotle University of Thessaloniki, Thessaloniki 54006, Greece
Tel: +30 2310 998778 Fax: +30 2310 998738 E-mail: thalex@agro.auth.gr

Abstract

One of the difficulties currently facing remote sensing scientists is the technical limitations of Earth Observation satellites, when trying to provide regular and fine resolution information about the water consumption of crops in irrigation systems. The solution could be to combine satellite images from various sources, some of high spatial resolution and others of high temporal resolution. In this study, actual evapotranspiration images from NOAA AVHRR acquired at various dates in Zhanghe irrigation district are used together with meteorological day reference evapotranspiration data to simulate day evapotranspiration. A temporal integration of day actual evapotranspiration for the May – September rice cropping season provides the seasonal actual evapotranspiration map. This information, collected at a pixel size of 1.1 km is merged together with a Landsat 7 ETM+ image acquired at a strategic moment of the cropping season. The result is a more detailed redistribution of seasonal evapotranspiration at a finer resolution, while keeping the actual evapo-transpired global volume constant, before and after the merging. This provides a better located estimation of water consumption, especially for rice. Irrigated rice fields are of particular interest to the water managers, since these fields are the main cash crop of the irrigation district. In the discussion that follows, it is shown that the remote sensing limitations can be overcome using meteorological data and combined information from two satellites, providing detailed results at a low cost.

1. Introduction

Balancing the limited water resources to match the human needs is a challenge to be faced in the coming years. Water resources have to be managed from the water basin to the irrigated crops, eventually reaching to smaller areas and users. Measuring the evapotranspiration is of the highest importance to understanding and eventually intervening into the water cycle of natural systems; especially in the water balance of the different critical users of water, such as irrigated areas. Remote sensing has been able, over the last 15 years, to provide methods for calculating the actual evapotranspiration (ETa) (Vidal and Perrier 1989; Bastiaanssen 1998).

A main limitation of the models used in remote sensing, is that they are based on a satellite image, representing the calculation of a day evapotranspiration. It would be tempting to process images every day if the computation procedures were not so intensive, and if optical satellite data were always cloud free and cost was not a limitation. As it is not so, most of the time, a limited amount of images processed into day evapotranspiration maps are available to supplement studies. The issue of temporal integration has been explored to fill in the missing data. Droogers and Bastiaanssen (2001) have worked on this aspect, improving the temporal and spatial variation of evapotranspiration from a water balance model by supplementing it with high-resolution satellite images of evapotranspiration. The satellite images provided the model with strategic calibration data to refine the seasonal estimation of the water balance for irrigated crops. Work performed by Bastiaanssen et al. (2002) and Bastiaanssen and Ali (2003) uses meteorological data to integrate ETa and crop growth, respectively, between satellite image data from the Indus Basin of Pakistan. Farah (2001) supplemented evaporation estimates from remote sensing over Kenya with coupled models of Penman-Monteith and Jarvis-Stewards to reconstitute evaporation under cloud conditions in the Navaisha Basin.

Despite the technological advance of remote sensors and the ability to detect finer objects on the ground, higher accuracy is always desirable. Technological restrictions confine satellite design to high resolution but low revisit frequency, or else low resolution and high revisit frequency. A combination of both qualities would be preferable, and therefore, techniques to merge satellite images of different spatial resolutions have been developed. Welch and Ehlers (1987) have used an Intensity-Hue-Saturation (IHS)

(Received 4 February 2002; Accepted 9 October 2003)
Asian Journal of Geoinformatics, Vol. 5, No. 1, September 2004
Published by ARSRIN, P.O. Box 4, Klong Luang, Pathumthani 12120, Thailand.

transformation to merge SPOT (Satellite Pour l'Observation de la Terre) panchromatic and Landsat multispectral satellite images, while Ambrosia et al. (1991) have used the same technique to merge airborne digital data with digitized aerial photography. Other techniques include the Principal Components transformation (Chavez et al., 1991), and merging of the spatial frequency content (Schowengerdt, 1980). Except for the need for spatial detail, another reason for this merge is that high resolution images are often costly, while low resolution are of low cost, or even are freely distributed. It is possible that remote sensing work can be performed using low-resolution satellite images that are later spatially enhanced using a high spatial resolution image.

In this study, the free-of-cost NOAA AVHRR (National Oceanographic and Atmospheric Administration – Advanced Very High Resolution Radiometer) images have provided a frequent source of data to calculate the volume of evapotranspired water that has been consumed over the Zhanghe irrigation district during the 2000 rice cropping season. A methodology is setup to:

- Calculate the seasonal ETa, a component estimated with difficulty in water balance studies.
- Develop an improved spatial resolution enhancement technique, applicable to the seasonal ETa map, using a single Landsat ETM+ (Enhanced Thematic Mapper Plus) image.
- Prove that the located estimations of water consumed for the whole season in rice fields can be enhanced through different scales.

2. Methods

2.1 Study Area

Situated in the Hubei Province, Central China, the Zhanghe irrigation district is located North of the Yangtze River (Changjiang). The net irrigated area reported is approximately 160,000 ha, accounting for a large proportion of Hubei Province's grain production. Rice production is widespread in the irrigation district, and the recent decline in water availability to agricultural purposes has not decreased the global rice production much, due to a proportional increase of efficiency of water use by the farmers (Dong et al., 2001). Even though the system is run under the main operation of the Zhanghe reservoir, there are thousands of small sized reservoirs, small basins and pump stations in Zhanghe irrigation district partly incorporated in the irrigation system, but sometimes operating independently (Loeve et al., 2001). The complexity of the system brings up the difficulty of quantifying by traditional scientific methods the volumes of water used.

2.2 Satellite Images

NOAA AVHRR LAC (Large Area Coverage) images were ordered and downloaded from the NOAA Satellite Active Archive (http://www.saa.noaa.gov). Five images of acceptable atmospheric conditions (no thermal anomalies and no identifiable clouds) were acquired. These covered the rice-cropping season of 2000 with an average representation period of 32 days. The dates of the satellite images are May 10, June 21, July 9, August 12, and September 15. These are pre- and post-date of the Landsat 7 ETM+ image, which was acquired on July 10 that is in the full period of rice crop. The satellites have inherent characteristics and advantages linked to their spatial resolution and revisiting periods (temporal resolution).

2.3 SEBAL Application in Zhanghe

The actual evapotranspiration was estimated with the Surface Energy Balance Algorithm for Land (SEBAL), which was developed by Bastiaanssen (1998). SEBAL is a thermodynamically based model, looking towards finding the energy-balance terms at the land surface. While involving a lot of empirically based steps, the physics at the core are robust thermodynamic equations. For insight of the practical procedure, Chemin et al. (2000) and Tasumi et al. (2000), provide extensive details of step-by-step considerations applied. It has been satisfactorily validated in many places and situations, from Spain (Bastiaanssen, 1995) to Pakistan (Bastiaanssen et al., 2001).

The evaporative fraction (Λ) is the output of SEBAL, and is defined as the ratio of latent heat to maximum net available energy (Equation 1)

$$\Lambda = \lambda E/(Q^*-G_0) = (Q^*-G_0-H)/(Q^*-G_0) \quad (-)$$

Equation 1

Where, Λ is the Evaporative Fraction, Q^* the instantaneous Net Radiation, G_0 the instantaneous Soil Heat flux, H the instantaneous Sensible Heat flux and λE the instantaneous Latent Heat of Vaporization. Λ can be interpreted in irrigated areas as the ratio of actual to crop evaporative potential; it is dependent on the atmospheric and soil moisture conditions equilibrium. In barren areas it can be interpreted as the residual evaporation of soil water available in the upper part of the soil profile. The soil heat flux G_0 used is defined as Equation 2:

$$G_0 = Rn \times \left[\frac{(T_0 - 273.15)}{\rho_0} \right] \times (0.0032 r_0 + 0.0062 r_0^2) \times (1 - 0.978 \times NDVI^4) \quad (W/m^2)$$

Equation 2

With r_0 the day time average surface reflectance it is ranging from 0.9 to 1.1 (Bastiaanssen, 1995). Parodi (2000), is referring to the term in the brackets as the proportion factor, describing the conductive heat transfer in the soil, while the remaining part (second line) is referred to as the extinction factor for the attenuation of radiation through canopies.

The Day Net Radiation is the electromagnetic balance of all incoming and outgoing fluxes reaching and leaving a flat surface (considered Lambertian in SEBAL) for the daylight hours (Equation 3, Bastiaanssen (1995)).

$$Rn_{Day} = (1-\rho_0) \times (K^{\downarrow}_{Day}) - 110 \times \tau_{sw} \quad (W/m^2)$$

Equation 3

where $K^{\downarrow}_{Day}$ is the incoming short-wave solar radiation (W/m^2), ρ_0 the surface albedo $(-)$, τ_{sw} is the day single-way transmissivity of the atmosphere (default = 0.7, or from meteorological data if available). The calculation of the evapotranspiration is including the transformation of Day Net radiation (Rn_{Day}) from W/m^2 to mm/day by the T_0 dependent latent heat of vaporization equation (Equation 4).

$$ET_a = \Lambda \times Rn_{Day} \times 86400.10^3$$
$$\times [(2.501-(0.002361 \times T_0)) \times 10^6]^{-1} \quad (mm/day)$$

Equation 4

where ET_a is the Day actual evapotranspiration, Rn_{Day} is the average day net radiation and T_0 the surface temperature.

Applying the SEBAL model to the Landsat ETM+ and NOAA AVHRR images of the Zhanghe irrigation district produces a set of intermediary products. These transitory layers of information are: the normalized difference vegetation index (NDVI), surface emissivity, surface albedo, surface temperature, radiative/conductive/convective energy fluxes at the soil surface, day potential ET and instantaneous evaporative fraction. Evaporation is calculated from the instantaneous evaporative fraction, and the day averaged net radiation. The evaporative fraction (Λ) is computed from the instantaneous surface energy balance at the moment of satellite overpass on a pixel-by-pixel basis. On the other hand, the day averaged net radiation is mainly dependent on surface black body radiation and on the sun incoming radiation heating the Earth surface, assimilated into a semi-empirical relationship (Equation 3). Climatic parameters used in the model are listed in Table 1 along with an indication on their estimated spatial variability within the study area.

The final product of the application of the SEBAL methodology on the Landsat ETM+ and NOAA AVHRR images are the ETa maps. According to the available literature, validation for the total coverage of the satellite image is not possible, since that would involve measurement of evapotranspiration or the individual energy fluxes in all the types of landcover that appear (Bastiaanssen et al., 1998). Instead, the values of the following variables are given for comparison in Table 2: the mean value of each ETa image, the value of ETa in the pixel of Tuanlin test site, the reference evapotranspiration (ET_0) calculated with the Penman-Monteith equation (Allen et al., 1998) and the crop evapotranspiration (ETc), which is the product of ET_0 multiplied with the crop coefficient (Kc) for the study area (Mao, 1992). The mean difference of ETa (SEBAL) and ETc (Penman-Monteith) is 0.84 mm/day. A possible reason for this difference is the lack of optimum conditions for rice growth, which is an assumption for the calculation of ETc. Moreover, measurements of the meteorological station are spatially specific, while the results of the SEBAL model refer to the mean evapotranspiration of all the types of land cover in each pixel, which for AVHRR sensor is 1.21 km^2. However, statistical comparison (paired T-test) has proven that this difference is non significant at the 0.05 level (P = 0.057), with 95% confidence interval -0.038 to 1.735. In addition, the correlation coefficient between the measurements and estimations is r = 0.983 (significant at the 0.05 level, P = 0.0026).

Moreover, the crop coefficient Kc was calculated for rice from the SEBAL model, and was compared to the values given in literature for the study area (Mao, 1992). Kc was calculated by dividing the ETa (SEBAL) value at the

Table 1: Climatic parameters used in the model

Parameter	Name	Unit	Spatial variability
Tmin	Minimum day temperature	K	Low-medium
TMax	Max day temperature	K	Low-medium
Tavg	Average day temperature	K	Low-medium
RH	Relative Humidity	%	Medium-high
U	Wind speed	m/s	Medium-high
τ_{sw}	Atmospheric transmissivity (single-way)	-	Low-medium

Table 2: Values of ETa, ET_0 and ETc at the Tuanlin location various sources (in mm/day)

Date of AVHRR image	ETa (SEBAL) mean value of image	ETa (SEBAL) value at Tuanlin location	ET_0 (Penman-Monteith) Tuanlin Met. Station	ETc (Penman-Monteith) Kc= 0.94 – 1.5 (Mao, 1992) Tuanlin Met. Station
10/5/00	3.8	3.5	4.0	3.8
21/6/00	4.5	4.7	4.3	6.0
9/7/00	5.4	5.4	4.1	6.2
12/8/00	6.3	6.1	5.6	7.8
15/9/00	3.0	2.9	3.1*	2.9

* Average of ET_0 from 1 to 10 September. There are no available data for dates after 10 September.

Tuanlin location with the ET_0 (Penman-Monteith) from the Tuanlin meteorological station (Figure 1). The values of Kc found in Mao (1992) are derived from experimental data of 30 stations, where evapotranspiration of rice was measured using nonweighing lysimeters. The lysimeters were made of concrete or other watertight material and had an area of 4 m^2 and a depth of 1.2 – 1.4 m. Monthly values are given for the rice cultivation period, and they refer to the greater area of Hubei province north of Yangtze river, which includes the study area. On the contrary, the Kc values estimated from the SEBAL model are spatially specific (they refer to the pixel of Tuanlin site) and temporally specific (they refer to the date of images acquisition). The larger difference of SEBAL estimated and cited in literature Kc in the middle of the rice growing season could be attributed to the above mentioned reasons.

2.4 Temporal Integration

Remote sensing calculation of ETa on certain sample dates during the cropping season gives a very good indication of its spatial distribution, but cannot be used directly in water balance studies. The reason behind is the wide fluctuation of ETa from day to day, depending on meteorological conditions and availability of water. Therefore, in order to obtain an accurate estimation of the seasonal ETa, daily values have to be simulated. A polynomial equation could describe the fluctuation of ETa, but a bigger sample of ET observations over time would be necessary to obtain an accurate result.

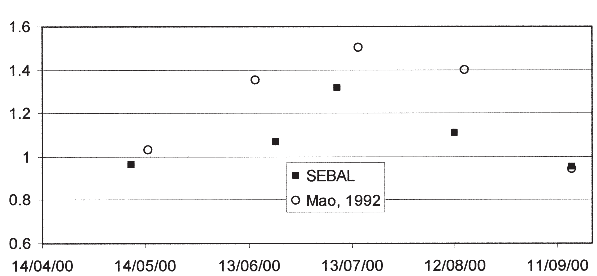

Figure 1: Comparison of crop coefficient Kc estimated using the SEBAL model with coefficient cited in literature (Mao, 1992).

Farah (2001) examined two methods for simulation of evapotranspiration during cloudy days, when optical remote sensing data cannot be acquired. The first method, which used the Penman-Monteith equation and Jarvis-Stewart model gave better results at small temporal steps than the second, which used Λ as an indicator of the level of soil moisture and assumed it as constant for the period between the satellite image acquisition. The study concluded, however, that if a high temporal detail is not necessary and the accumulated ETa of seven or more days is adequate, the Λ method is advisable for operational applications due to its simplicity. Moreover, it was suggested that a weekly temporal step of satellite image acquisitions is adequate for the studied area in Kenya.

In this study, the missing time component was provided by daily calculation of ET_0 (reference evapotranspiration) as proposed by Tasumi and Allen (2000). ET_0 was calculated with the standardized Penman-Monteith method (Allen et al., 1998). Similar to Farah's Λ method, the fraction $c_j = ETa/ET_0$ was considered constant for the time period j between two consecutive satellite images, and the daily ETa could be simulated with the Equation 5:

$$ETa' = c_j \, ET_0 \qquad \text{Equation 5}$$

where ETa′ are the daily simulated ETa maps. Equation 5 is using the time component (ET_0) to calibrate the spatial component of ETa calculation (c_j) in order to better describe the daily fluctuation, which is dependent on meteorological conditions. ETa also depends on the availability of water. Spatial variation of water availability can be described by the five ETa maps, which were assumed representative for each period j.

After the simulation of daily ETa', the values for the whole season were integrated and the seasonal ETa (ETs) is calculated on a pixel basis:

$$ETs = \sum_{t_1}^{t_2} ETa' \qquad \text{Equation 6}$$

where t_1 to t_2 is the period from May 01 to September 10, 2000.

The good spatial distribution of the satellite image is not matched with equally good meteorological data. Unfortunately there is only one meteorological station in Zhanghe, in the center of the irrigated area, and is not representative of the climatic conditions present in the area. Nonetheless, the measurements from the meteorological station were considered uniform across the Zhanghe irrigation district, due to lack of other data. The study area is of undulating light slope terrain, with rice crops in depressions and other crops on higher grounds. There seems to be some East to West wind in the summer season, that can make clouds pass over the whole study area within a day or more than a day. This can influence all climatologic parameters to some extents that are not estimated here. Spatially related inaccuracies maybe propagated from instantaneous to day values, in the case of haze/clouds, the later more common in Zhanghe. Over a day, probable inaccuracies in spatial distribution of ETa may arise for the above-stated reasons, but when integrating in time, those spatial inaccuracies may reduce largely (some elements inferring this can be found in Bastiaanssen et al., 2002), especially when considering the long term variations of atmospheric transmissivity that contributes to the day net radiation estimation in SEBAL.

The above mentioned limitations are expected to insert a certain amount of error in the estimation of the seasonal evapotranspiration. Installation of lysimeters in the study area would have provided a source of data for validation, but with a significant cost increase.

2.5 Resolution Improvement

The spatial resolution of ETs estimated in the previous paragraph is limited by the resolution of NOAA AVHRR satellite images (1.1 km at nadir). Alexandridis and Chemin (2001) after performing multiple scale analysis in the same dataset, concluded that higher resolution would be desirable in the Zhanghe irrigation district because of the size of the fields (about 2×1.5 m), and the texture of the cropping pattern. This can be achieved by using the higher spatial resolution of the available Landsat ETM+ satellite image (30 m). The detailed pattern of the ETa map is used as a weight to spatially redistribute the ETs calculated for each 1.21 km^2 pixel of the NOAA AVHRR satellite using the formula:

$$ETs' = ETs \cdot \frac{ET_{ETM+}}{\left(ET_{ETM+}\right)} \qquad \text{Equation 7}$$

where $\overline{ET_{ETM+}}$ is the average of the values of ET_{ETM+} (Landsat) that occupy a pixel of ETs (NOAA).

Using this proportional distribution method, the total ETs value calculated for each area of 1.21 km^2 is preserved, but redistributed according to the detailed pattern of ETa derived from the ETM+ image. In this way, the influence of the high-resolution image induced in the methods found in literature (IHS and PC transformation) is avoided.

The resulting ETs′ image using this method has a 'blocky' appearance, with block size of 1 km, similar to the original ETs image. This interference of the original image only degrades the visual appearance of the resulting image, while locally the values of the pixels are correct, since this method simply redistributes the values without altering them. The 'blocky' appearance is more intense in areas where the ETa_{ETM+} image does not satisfactorily represent the spatial pattern of the seasonal evapotranspiration.

Following Ambrosia et al. (1991), who suggest that a spatial resolution difference factor of 36 would be excessive (from 1.1 km to 30 m), factors of 2 and 4 have been used in order to redistribute the ETa values to spatial resolutions of 500 m and to 250 m, respectively.

2.6 Elements of Validation

According to Zhou et al. (1998) no method is available for absolute evaluation of the result of resolution improvement. Thus, the results of this method were compared with the results of another method, already used by Bastiaanssen et al. (2001). This second method produces the resulting image based on the high resolution data, normalizing them at an image level and not at a pixel level:

$$ETs' = ETa_{ETM+} \cdot \frac{\overline{ETs^{image}}}{\overline{ETs^{image}_{ETM+}}} \quad (mm/season) \qquad \text{Equation 8}$$

where $\overline{ETs^{image}}$ is the mean of the ETs image and $\overline{ETs^{image}_{ETM+}}$ is the mean of the ETa image calculated from the ETM+ sensor.

Using the second method, the values of ETa which were calculated from the ETM+ image, were normalized using the coefficient $\frac{\overline{ETs^{image}}}{\overline{ETs^{image}_{ETM+}}}$. This method assumes that the spatial distribution of a single day ETa is representative of the spatial distribution of ETs of the rice growing season, which is not always true.

The quality comparison of the images produced by the two methods was performed according to Zhou et al. (1998). More specifically, the spectral quality, which is the level at which the produced images retain the pixel values of the original image, was checked by comparing the absolute differences of the resulting images with the original image, at a pixel level. The results favor the first method, which has the lowest absolute difference. The spatial quality, which is the level at which the produced images retain the spatial information of the high resolution image, was checked by comparing the correlation coefficients of each produced image with the ETa_{ETM+} image. The comparison of the correlation coefficients favor the second method. The results are presented in Table 3.

Table 3: Spectral and spatial comparison of the two resolution improvement methods

	Spectral quality (mean absolute difference with original ETs)	Spatial quality (correlation coefficient with ETa_{ETM+})
Method 1 (new)	29.9	0.90
Method 2 (Bastiaanssen et al., 2001)	35.7	0.99

Further work using this method by Chemin et al. (2003) has resulted in some additional elements for validation. A set of two water depletion and two water productivity indicators have been calculated with the rice ETs values from the remote sensing according to this paper's method. Ground data of rice ETs was calculated by the method found in Allen et al. (1998) with local meteorological data (Dong et al., 2001). Results of the summer 2000 rice season for an irrigated area of 300 hectares show 1% difference for each of the two water depletion indicators, while results for the two water productivity indicators show <1% and 15%. ETs difference between ground data and this RS method is 1%.

3. Results and Discussion

Simulation of day ETa raster maps was accomplished using Farah's (2001) Λ method, described in the previous paragraphs. After the integration of the maps on a pixel-by-pixel basis, the seasonal ETa map (ETs) was produced. The ETs map describes the amount of water consumed (evapo-transpired) per unit area during the cropping season of rice (1 May 2000 – 10 September 2000), in the Zhanghe irrigation district (Table 4). Even with the 1.1 km spatial resolution (Figure 2 (a)), the dryer non-irrigated areas (light tones of gray) can be differentiated from the areas where irrigated fields prevail (darker tones of gray).

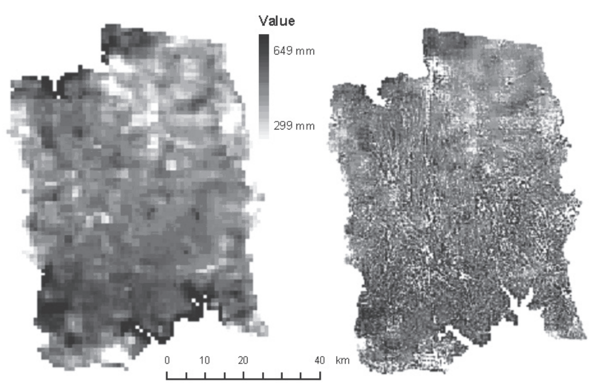

(a) (b)

Figure 2: Seasonal actual evapotranspiration (ETs) map of Zhanghe irrigation district (1.1 km and 250 m)

Table 4: Seasonal evapotranspiration (ETs) in Zhanghe irrigation district

Area	444300 ha
Global volume of water	2.0963 km^3
Mean ETs	472 mm/season
Min. ETs	299 mm/season
Max. ETs	649 mm/season

The spatial resolution of the ETs map was improved with the use of a newly presented method, and compared with the result of another method, already in use. Although the spatial quality of the existing method is slightly higher, the new method presents a higher spectral quality, which means that the original spatial distribution of ETs is preserved at a higher degree.

The 250 m pixel size map, which was enhanced using the new method, is presented in Figure 2 (b). Clearly, a different pattern is visible with interesting string type features that are the lowland rice cropping areas (dark gray). Lower ETs (light gray) is found in the natural vegetation interweaved between the rice features. An enlarged detail from Zhanghe irrigation district is shown in Figure 3, where the pattern of irrigated areas (dark gray) gradually becomes more visible.

The global volume of water consumed in Zhanghe irrigation district is given in Table 5, calculated in different spatial resolutions. The mean value for the whole map is constant, as expected, since only the distribution of the values has changed to a more detailed pattern. For the same reason the standard deviation of the ETs map increases when moving to finer resolution. The global volume of water seems to change with the change of resolution; this is due to the appearance of clouds in the high resolution Landsat image. A cloud mask was manually delineated based on the combination of thermal and visible bands in the Landsat scene. The mask was used to remove the clouds

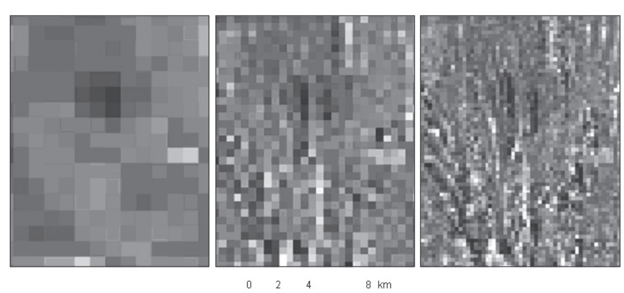

(a) (b) (c)

Figure 3: Area of ETs map in various spatial resolutions (1.1 km, 500 m and 250 m)

and varies slightly with the resampling effect through pixel size. The cloud covered area changes and influencing the remaining cloud-free area, and therefore alters the global volume of water consumed.

Spatial distribution of the water consumed has improved, leading to higher ETs accuracy per land class. The same image (Landsat 7 ETM+) was used for the land use map and for the high resolution ETa map, therefore the spatial coincidence is absolute, and need for validation became obsolete. The major irrigated crop in Zhanghe is rice, covering 33% of the area. Statistics for rice covered areas (Table 6) indicate a small increase in mean ETs when spatial resolution becomes finer. The improvement of the spatial distribution of the ETs through smaller pixel sizes separates more and more the low consumptive land classes from the highly consumptive irrigated rice areas. Therefore less influence from other land classes is input when calculating statistics for rice, and the refined result reaches ideally towards pure rice pixels only. Nevertheless, the mean ETs for rice areas is not significantly higher than the mean of the total area, which leads to the conclusion that other features are equally high in water consumption as rice. These could be the open water bodies, which are numerous in the area, or other irrigated crops, such as cotton. The levels of standard deviations are smaller in the rice areas (Table 6) than the overall Zhanghe assessment (Table 5). This is expected because rice land use class has homogeneous NDVI, albedo and temperature responses. As a result, less variation is observed among rice pixels within ETa (thus ETs) maps, than other more heterogeneous land use classes.

4. Conclusions and Limitations

Simulation of day ETa and temporal integration was used to estimate the volume of water consumed during the rice cropping season (ETs). A source of insecurity in this estimation was the monthly time step between the NOAA AVHRR images. Its estimation would improve if more frequent images were acquired, at a 10 or 15 days step. A method for validation of this result would demand the installation of a series of lysimeters or scintillometers, with an excessive cost beyond the resources of this study.

The ETs map is produced in the original spatial resolution of NOAA AVHRR (1.1 km). Improving the spatial resolution of ETs map is possible by using additional high resolution information, which is derived in this case from a Landsat ETM+ ETa map. A new method was proposed which redistributed the pixel values of the ETs map proportionally to the high resolution ETa map (Landsat ETM+). The method was compared to an existing method already used in large geographic scale studies. The comparison revealed a higher spatial quality of the existing method and a higher spectral quality of the new method. Since the correct re-distribution of the original values was considered important, the new method was adopted.

Another subject which could limit the validity of the results was considered: the issue of representativity of a single day ETa map (10 July 2000) for the whole rice cropping season (1 May 2000 – 10 September 2000). The values of ETs measured for the whole season have been redistributed within each pixel proportionally to the use of

Table 5: ETs in Zhanghe at different spatial resolutions

Spatial resolution	Area (ha)	Global volume of water (km^3)	Mean ETs (mm/season)	Standard deviation (mm/season)
1.1 km	444300	2.0963	472	33
500 m	438225	2.0680	472	45
250 m	438737	2.0677	472	55

Table 6: ETs in rice covered areas at different spatial resolutions

Spatial resolution	Area (ha)	Global volume of water (km^3)	Mean ETs (mm/season)	Standard deviation (mm/season)
1.1 km	142900	0.6768	474	24
500 m	144200	0.6915	480	36
250 m	144800	0.7048	487	44

water on a single day. The land use does not change within the same cropping season, and therefore variation of evapotranspiration between irrigated areas, natural vegetation, settlement areas and other land uses, can be correctly described. Within irrigated areas, a degree of inaccuracy in the redistribution of ETs is expected since the rate of evapotranspiration changes during the cropping cycle. Nevertheless, a degree of representation is provided since the chosen day is when rice is at full maturity and therefore fully evapo-transpiring. Use of another high resolution image acquired at a different stage of the rice growing season could improve the results of the resolution improvement procedure.

The simulation of temporal detail and then the improvement of location accuracy of ETs do bring a good trade off in low-cost water consumption monitoring of irrigation systems of medium areas. The redistribution of ETs preserves the original estimated water volumes from NOAA AVHRR, but improves the allocation of water used between different land use classes, especially irrigated versus non-irrigated, since it is of first interest to water managers in an irrigation system *a priori*. The improved ETs of the high water consumption irrigated crops (rice) can be further derived for primary and secondary canals if necessary. This allows the water managers to assess more accurately the performance and the water balance of irrigation subsystems under operational constraints. Improvement of the water efficiency at different levels of water supply and distribution can find suitable support in such technique for planning processes. The enhanced information content at a low cost is very attractive for water managers and decision support system applications, especially in the sub-system level of irrigated areas where high resolution ET data is not spatially and temporally available simultaneously.

References

Alexandridis, T., and Chemin, Y., 2001, Irrigation water consumption through remote sensing. Comparison at different scales in Zhanghe irrigation system, China. *Presented in First International Conference on Water Resources Management, Halkidiki,* Greece, 10pp.

Allen, R.G., Pereira, L.S., Raes, D., and Smith, M., 1998, Crop evapotranspiration. *Guidelines for computing crop water requirements.* FAO irrigation and drainage paper No 56. FAO, Rome, 300pp.

Ambrosia, V.G., Myers, J.S., Ekstrand, R.E., and Fitzgerald, M.T., 1991, Integration of Airborne Thematic Mapper Simulator (TMS) data and digitised areal photography via IHS. *Geocarto International,* 6(2), 45-48.

Bastiaanssen, W.G.M., 1995, Regionalization of surface flux densities and moisture indicators in composite terrain. A remote sensing approach under clear skies in Mediterranean climates. *Agricultural Research Department, Report 109,* Wageningen, The Netherlands.

Bastiaanssen, W.G.M., 1998, *Remote sensing in water resources management: the state of the art*. International Water Management Institute (IWMI), Colombo, Sri Lanka.

Bastiaanssen, W.G.M., Pelgrum, H., Wang, J., Ma, Y., Moreno, J.F., Roerink, G.J., and van der Wal, T., 1998, A remote sensing surface energy balance algorithm for land (SEBAL), 2. Validation. *Journal of Hydrology.* 212-213: 213-229.

Bastiaanssen, W.G.M., Brito, R.A.L., Bos, M.G., Souza, R.A., Cavalcanti, E.B., and Bakker, M.M., 2001, Low cost satellite data for monthly irrigation performance monitoring: Benchmarks from Nilo Coelho, Brazil. *Irrigation and Drainage Systems,* 15: 53-79.

Bastiaanssen, W.G.M., Ahmad, M.D., and Chemin, Y., 2002, Satellite Surveillance of water use across the Indus Basin. *Water Resources Research,* 38(12), 1273.

Bastiaanssen, W.G.M., and Ali, S., 2003, A new crop yield forecasting model based on satellite measurements applied across the Indus Basin, Pakistan. *Agriculture, Ecosystems and Environment,* 94(3), 321-340.

Chavez, P.J., Sides, S.C., and Anderson, J.A., 1991, Comparison of three different methods to merge multiresolution and multispectral data: Landsat TM and SPOT panchromatic. *Photogrammetric Engineering and Remote Sensing,* 57(3), 295-303.

Chemin, Y., Alexandridis, T., and Loeve, R., 2003, Water productivity at different spatial scales from remote sensing. Zhanghe Irrigation District, Hubei Province, China. *Journal of Irrigation Science,* submitted.

Dong, B., Loeve, R., Li, Y.H., Chen, C.D., Deng, L., Molden, D.J., 2001, Water productivity in Zhanghe Irrigation System: Issues of scale. In: Barker R, Loeve R, Li YH, Tuong TP (eds) Water-saving irrigation for rice: *Proceedings of an International Workshop held in Wuhan,* China 23-25 March 2001 International Water Management Institute, Colombo, Sri Lanka, pp.97-115.

Droogers, P., and Bastiaanssen, W.G.M., 2001, Combining remote sensing and hydrological models to enhance spatial and temporal variability. Remote Sensing and Hydrology 2000. (Proceedings of a symposium held at Santa Fe, New Mexico, USA, April 2000). *IAHS Publ. no.* 267, 574ñ579.

Farah, H.O., 2001, *Estimation of regional evaporation under different weather conditions from satellite and meteorological data: a case study in the Navaisha Basin, Kenya.* Doctoral Thesis Wageningen University and ITC, CIP-Data Koninklijke Biblotheek, Den Haag, The Netherlands, 170pp.

Loeve, R., Dong, B., and Molden, D.J., 2001, *Operation of the Zhanghe Irrigation System.* In International Workshop on Water Saving Irrigation for Paddy Rice, 23-25 March 2001, Wuhan, China. China Rural Water and Hydropower. pp.95-115.

Parodi, G., 2000, *AVHRR Hydrological Analysis System – Algorithms and theory – Version 1.0.* WRES, ITC, The Netherlands.

Schowengerdt, R.A., 1980, Reconstruction of multispatial, multispectral image data using spatial frequency content. *Photogrammetric Engineering and Remote Sensing,* 46(10), 1325-1334.

Tasumi, M., and Allen, R.G., 2000, Application of the SEBAL methodology for estimating consumptive use of water and streamflow depletion in the Bear River Basin of Idaho through Remote Sensing. Appendix A: The theoretical basis of SEBAL. *Final Report. The Raytheon Systems Company,* EOSDIS Project.

Tasumi, M., Bastiannssen, W.G.M., and Allen, R.G., 2000, Application of the SEBAL methodology for estimating consumptive use of water and streamflow depletion in the Bear River Basin of Idaho through Remote Sensing. Appendix C: A step-by-step guide to running SEBAL. *Final Report. The Raytheon Systems Company,* EOSDIS Project.

Vidal, A., and Perrier, A., 1989, Analysis of a simplified relation used to estimate daily evapotranspiration from satellite thermal IR data. *International Journal of Remote Sensing,* 10(8), 1,327-1,337.

Welch, R., and Ehlers, W., 1987, Merging multiresolution SPOT HRV and Landsat TM data. *Photogrammetric Engineering and Remote Sensing,* 53(3), 301-303.

Zhou, J., Civco, D.L., and Silander, J.A., 1998, A wavelet transform method to merge Landsat TM and SPOT panchromatic data. *International Journal of Remote Sensing,* 19(4), 743-757.

Yann Chemin got his M.Sc. in Land and Water Resources Management from Silsoe College (UK), he is currently following his research period as Doctorate Student in the Asian Institute of Technology (Thailand). His research interests are in evapotranspiration by remote sensing and RS supercomputing.

Thomas Alexandridis received his BSc in Agricultural Engineering from the Aristotle University of Thessaloniki (Greece). His specialization in the field of Applied Remote Sensing started with a Masters Degree at Cranfield University/Silsoe College (United Kingdom) and continued with a PhD at the Faculty of Agriculture, Aristotle University of Thessaloniki (Greece). Since then, he has been participating in research projects, carrying out consultancy work for research institutes and private companies, and is also a part-time lecturer in a Technical University. His research interests are environmental monitoring and modeling, Water resources management, and multiple scale issues in remote sensing and GIS.